Compact Transponder Front-End with Enhanced Gain for Electronic Toll Collection at 5.8 GHz

Stefano Maddio [1], Alessandro Cidronali [2], Marco Passafiume [3], Giovanni Collodi [4], Gianfranco Manes [5]
Dept. of Information Engineering, University of Florence, V.S. Marta, 3, I-50139, Florence, Italy
{ [1]stefano.maddio, [2]alessandro.cidronali, [3]marco.passafiume, [4]giovanni.collodi, [5]gianfranco.manes}@unifi.it

***Abstract*—In this paper we present a compact semi-passive front-end designed for Dedicated Short Range Communication (DSRC) at 5.8 GHz for vehicular technology applications. The front-end implementation is based on the optimal integration of a low-bias RF diode and a compact circular polarized antenna array.**

The antenna array natively exhibits the optimum termination to the diode, ensuring the best trade-off between detection and back-scattering on the basis of frequency conversion mechanism. The antenna is characterized by enhanced gain and polarization purity while extremely compact, hence particularly suitable for tag integration.

The fabricated prototype is tested in envelope detection, back-scattering and in a functional test conducted according to the ETSI EN300674 communication layer. The best measured Back-Scattering gain exceeds 7.8 dB, with a sensitivity of 54 mVpp with a signal of -45 dBm. A range at 9 m without communication errors is observed when operating with a EIRP of 33 dBm.

Keywords*—Transponder, back-scattering, vehicular communication, circular polarization antenna

I. Introduction

In the framework of Intelligent Transportation System, European Telecommunications Standards Institute (ETSI) technical committee recommends Dedicated Short Range Communication (DSRC) in the 5.8 - 5.9 GHz band operating in Circular Polarization (CP) [1]. For the application of Electronic Toll Collection (ETC), the fixed equipment, known as Road Side Unit (RSU), is expected to communicate with compact semi-passive mobile unit, indicated as One Board Unit (OBU).

The OBU architecture is mainly based on passive transponder. This is due to the extremely low DC power consumption requirements that makes unsuitable the use of even low-power consumption local oscillator [2]. While OBU passive transponder front-end design based on antenna pair are already available [3], the solutions based on a single antenna are more convenient for the sake of device compactness, [4], [5]. Single antenna front-end operation is based on the Back-scattering mechanism, where a RF diode operates the frequency conversion with the receivingtransmitting antenna [6].

Figure 1 depicts the operation principle of the tag, which operates as follows. In the down-link (DL), the RSU sends messages by an amplitude shift keying (ASK) modulated carrier; the OBU front-end operates as an envelope detector, while the OBU base-band processor decodes the demodulated waveform into a bit stream. In the up-link (UL), the OBU semi-passive transponder front-end works as a back-scatterer, [3], [7], impressing a BPSK modulated sub-carrier onto the received carrier by an ASK modulation.

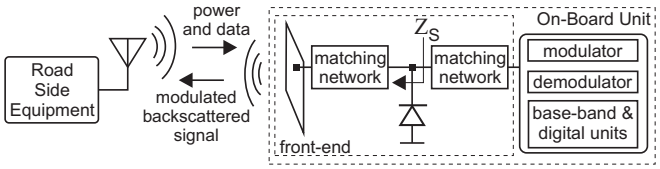

Fig. 1: On Board Unit Operation principle

The native integration of antenna and diode avoids both power loss and spurious radiation which can be severe operating at the central frequency of 5.8 GHz, especially considering lossy substrates such as FR4. The antenna is assumed as a linear time-varying load in both Upload (UL) and Download (DL) states. Therefore the optimum design has to deal with the optimal balance between sensitivity and output power in order to maximize the operative range.

While the design of single CP antenna with arbitrary input impedance is challenging, but not impossible [8], [9], the sequential array architecture [10] offers more versatility and intrinsic advantages such as gain enhancement and higher polarization purity. The only issue is the demand of a larger area, which is in contrast to the requirement of small dimension for the OBU.

In this paper we apply the ultracompact design proposed in [11] to the optimal detector design described in [6], resulting in a very compact single layer design of 40 mm×40 mm, enabling an easy integration with the existing back-end. The experimental validation of a prototype designed around the optimal trade-off confirms the proposed approach, exhibiting a sensitivity of 54 and a back-scattering gain of 7.8, which translate in a communication range of 9 m free from error when operating according to ETSI EN300674 communication layer.

II. Transponder Conversion Analysis

We focus on the BAT15-03W low-bias RF diode biased with a 4μ A current as in [6]. For the goal of this investigation, the RF diode is assumed to be driven by two signals, respectively the small-signal, centered at ω_s, and the large-signal, centered at ω_p. Considering the classic conversion matrix theory [12], the frequency conversion occurring at the transponder front-end in the UL and DL modes is characterized by the corresponding admittance conversion matrices of the RF diode, $\mathbf{Y_{UL}}$ and $\mathbf{Y_{DL}}$, which can be extracted analytically once the the diode is accurately characterized, or by measurement

as described in [13]. The diode is fully characterized on the basis of the large-signal model provided by the vendor, as well as with the actual package parasitics description.

In the UL, the large-signal is represented by the base-band modulating signal, the RF carrier being the small-signal one. In the DL, the large-signal is assumed to be the carrier frequency, while the side bands, determined by the ASK modulation at the RSU, represent the small-signal tone. Since small-signal analysis is linear, it is possible and convenient to write the mixing frequencies as $\omega_n = \pm\omega_s + n\omega_P$.

The following expressions model the analytical relations between the phasors of current and voltage of the mixing diode.

$$\begin{vmatrix} I_d(\omega_{rf}+\omega_{bb}) \\ I_d(\omega_{bb}) \end{vmatrix} = \mathbf{Y_{DL}} \begin{vmatrix} V_d(\omega_{rf}+\omega_{bb}) \\ V_d(\omega_{bb}) \end{vmatrix} \quad (1)$$

$$\begin{vmatrix} I_d(\omega_{rf}) \\ I_d(\omega_{rf}+\omega_{bb}) \end{vmatrix} = \mathbf{Y_{UL}} \begin{vmatrix} V_d(\omega_{rf}) \\ V_d(\omega_{rf}+\omega_{bb}) \end{vmatrix} \quad (2)$$

where ω_{rf} is the angular frequency of the RF carrier and with ω_{bb} is the modulating base-band signal.

The direct application of linear analysis to the two-port devices represented by $\mathbf{Y_{UL}}$ and $\mathbf{Y_{DL}}$ provides the back-scattering gain in UL and the sensitivity in DL.

Assuming a carrier at 5.8 GHz which is ASK-modulated by a tone at 500 kHz with a modulation index of 0.5, with an impinging power ranging from -43 dBm to -20 dBm, the calculated conversion matrix $\mathbf{Y_{DL}}$ is:

$$\mathbf{Y_{DL}} = \begin{vmatrix} (0.66+\mathrm{j}\,3.80) & (3.08+\mathrm{j}\,4.09) \\ (0.59+\mathrm{j}\,3.48) & (0.02+\mathrm{j}\,3.25)\cdot 10^{-2} \end{vmatrix} \cdot 10^{-2} \quad (3)$$

Therefore, the optimum impedances matching simultaneously the source (antenna) and the load (BB unit), and thus providing the maximum transponder sensitivity, are $Z_{S_{DL}} = 4.1 + \mathrm{j}\,25.2\Omega$ and $Z_{L_{DL}} \approx 6000 + \mathrm{j}\,0\Omega$.

Similarly, in the UL state, the diode is driven by the base band processor with a 300 mVpp square waveform switching the diode between the OFF and ON states at 2 MHz. Again, the conversion matrix $\mathbf{Y_{UL}}$ can be calculated as:

$$\mathbf{Y_{UL}} = \begin{vmatrix} 1.67+\mathrm{j}\,0.40 & 1.49-\mathrm{j}\,1.30 \\ -1.49+\mathrm{j}\,1.30 & 1.67+\mathrm{j}\,0.39 \end{vmatrix} \cdot 10^{-2} \quad (4)$$

From these matrices, we derive the optimum impedances matching the source and the load, providing the maximum conversion gain, which are $Z_{S_{UL}} = 55.2 - \mathrm{j}\,28.2\Omega$ and $Z_{L_{UL}} \approx 55.1 - \mathrm{j}\,28.4\Omega$.

The two terminations, $Z_{S_{UL}}$ at ω_{RF} and $Z_{S_{DL}}$, at $\omega_{RF} + \omega_{bb}$, are significantly different, while $Z_{L_{UL}}$ is close to $Z_{S_{UL}}$, thanks to the proximity of input and output frequencies. The base-band termination in the DL case presents a very high impedance $Z_{L_{DL}}$, as expected for envelope detection.

The calculated $\mathbf{Y_{DL}}$ and $\mathbf{Y_{UL}}$ permits to estimate maximum conversion gain of -4.4 dB for the UL state, and the maximum sensitivity of 23 mV/μW at -43 dBm for the DL state.

III. Antenna Design

ETSI recommends CP operation with at least 15 dB of cross-polarization level [1]. Among the existing solutions, the modal degeneration technique is effective in ensuring compact size and adequate polarization purity [14]. Figure 2a depicts a disc patch antenna centrally slitted by an elliptical cut. The cut operates as the degeneration driver splitting the fundamental TM_{11} mode into two similar but slightly detuned ones – labeled as TM_{x} and TM_{y}– due to the differently forced modal current paths [14], [9], [15].

According to the cavity model theory, the two modes are the sources of two geometrically orthogonal Linear Polarized (LP) far-fields, exhibiting an input impedance response which can be written as [9], [15]:

$$Z_{x/y}(\omega) = \frac{R_{x/y}}{1+\mathrm{j}\,Q\left(\frac{\omega}{\omega_{x,y}} - \frac{\omega_{x,y}}{\omega}\right)} \quad (5)$$

Where the equivalent circuital parameters $R_{x/y}$, Q and $\omega_{x/y}$ depend on the actual geometry of the patch (radius and ellipse dimensions) and on the substrate characteristics [8], [9], [15].

Controlling the parameter set and the input angle – the angle the input line identifies respect to the ellipse major axis – it is possible to obtain nominal CP and arbitrary input impedance at desired central system frequency [8], [15]:

$$\begin{cases} Z_{in}(\omega) = Z_x(\omega) + Z_y(\omega) \\ AR(\omega) = {}^{Z_y(\omega)}/_{Z_x(\omega)} \end{cases} \quad (6)$$

It can be observed that the Axial Ratio (AR) is proportional to the ratio of the two resonant modes and the complete input impedance is the sum of two modal responses. A front-end for an ETSI complaint OBU based on on this approach was proposed by the authors in [3].

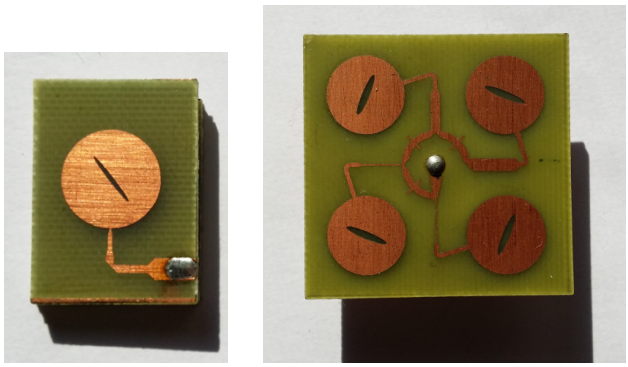

(a) Basic Element (b) 2 × 2 Sequential Array

Fig. 2: Compact Elliptical Slitted Disc Antennas.

However, for cheap lossy substrate – such as FR4 – it is difficult to exceed 4 dB of gain. In addition, the dispersion of the dielectric characteristics affects the precise conditions for the modal recombinations, deteriorating the polarization purity.

To enforce the polarization and enhance the gain at the same time, a compact 2 × 2 array configuration is considered. The Sequential Phase Architecture [10] is a valid aid to

enhance polarization purity and gain at the same time. It is based on the Sequential Phase Network (SPN), a beam-forming network operating as 90° phase-shifting power divider. The nominal design rules recommend a inter-element distance of $0.7\lambda_0$, which unfortunately cannot be met with the size constraints of mass-produced OBU's, for which the area reserved to the antenna is about 40 mm×40 mm [10].

In [11] a novel SPN based on compact curved design was proposed. The array in Fig. 2b is synthesized applying the cited design to the element in Fig. 2a. A CP gain exceeding 6 dB even constraint in the 40 mm square PCB is obtained. At the same time, tuning the impedance transformation operated by the SPN, which operates also as matching network, the resultant array termination can be adapted to the diode load requirement.

IV. Optimal Integrated Design

The optimal back-scattering front-end is achieved integrating the antenna array with the RF diode, when the former input impedance is seen as the optimal termination for the latter.

We assume that the RF diode is matched to $Z_{L_{UL}}$ at $\omega_{RF}+\omega_{bb}$ and to $Z_{L_{DL}}$ at ω_{RF}, therefore, recalling the conversion matrix analysis in Section II, the matrices in (1) and (2) permit to calculate the conversion gain isoclines for the entire real impedance domain, represented in a standard smith chart in Fig. 3 [6]. The DL and UL operation modes culminate in the two poles $Z_{S_{UL}}$ and $Z_{S_{DL}}$ representing the best conversion gain and the best sensitivity.

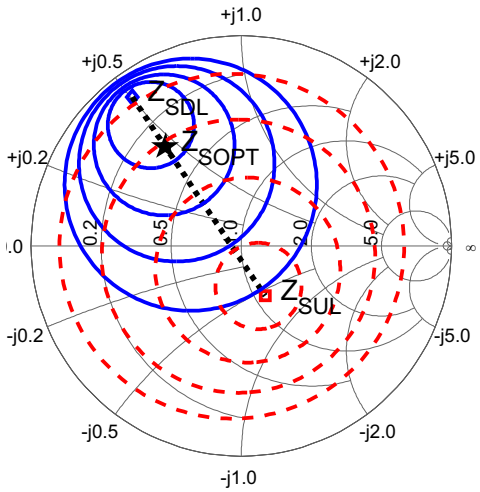

Fig. 3: Loci for available gain and sensitivity. The best terminations $Z_{S_{DL}}$ and $Z_{S_{UL}}$ are highlighted as well as trade-off frontier, where the optimal impedance $Z_{S_{opt}}$ is located. Isocline spacing: 2 dB gain for UL and 8 mV/μW for DL.

The dotted line in Fig. 3 represents the best frontier for the DL-UL trade-off, therefore the optimal system termination $Z_{S_{opt}}$ must lie here, in a position satisfying both the constraints of UL and DL [6]. To determine the actual value of this termination, the system constraints must be considered. A simplify model for the round-trip power budget is:

$$\begin{cases} EIRP - Loss + G_A \geq OBU_{\text{sens}} & \text{for the DL} \\ EIRP - 2 \cdot Loss + G_{BS} \geq RSE_{\text{sens}} & \text{for the DL+UL} \end{cases} \quad (7)$$

Where EIRP, the effective isotropic radiated power for the RSU, is 33 dBm, RSE_{sens} and OBU_{sens}, the RSU and OBU sensitivity, are -105 dBm and -43 dBm, respectively, and $G_{BS} = (2\,G_A + G_C)$, with G_A power gain of the antenna.

Following the method in [6], and considering the conservative constraint of a maximum distance of 7 m. hence a Loss of 65 dB, and a minimum antenna gain G_{ant} = 4 dB, the termination for the optimal trade-off is $Z_{S_{opt}} = 16 + j23\,\Omega$.

Therefore, the antenna design investigated has to exhibit an input impedance proximate to $Z_{S_{opt}}$, with the higher gain possible. The amount of tolerance can be straightfully understood inspecting the isoclines in Fig. 3

V. Prototype Fabrication and Experimental Validation

A sequential antenna array was optimized to maximize the gain at 5.8 GHz. Figure 4 depicts the final prototype designed after a system optimization having for goal the gain maximization with the best matching for the $Z_{S_{opt}}$ impedance found in the previous section. The front-end is printed with standard photo-etching procedure and then assembled with the base-band processor: the RF diode is placed at the beginning of the SPN, at the center of the PCB. The prototype is then tested to confirm the validity of the proposed design.

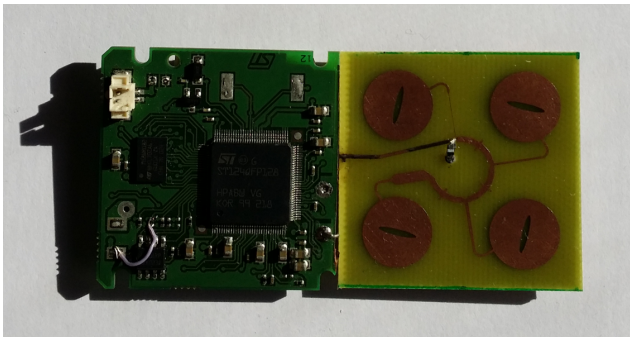

Fig. 4: Fabricated prototype in microstrip technology (FR4) assembled with the base-band processor.

The goal of first test is to verify the DL mode at the four carrier frequencies between 5.7975 and 5.8125 GHz, as specified by ETSI CEN-TC278 communication protocol for this class of devices. The obtained back-scattering Gain is depicted in Fig. 5a. The test signal consists in a continuously repeated *1-0* ASK sequence encoded with 500 kbps FM0. The device is forced to be in a permanent wake-up state, to increase the measurement accuracy.

In Fig. 5b the collected voltage waveform, expressed as RMS value, for incident power waves in the range [-21 dBm – -45 dBm] are presented. The error bars indicate the dispersion of the measured voltage among the four carriers. The sensitivity is estimated as 47 mV / μW for at -43 dBm.

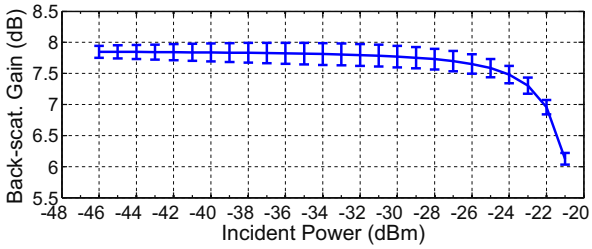

(a) Back-scattering gain versus incident power.

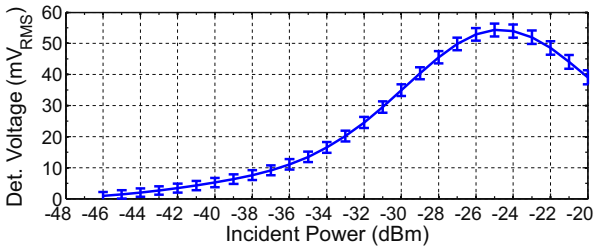

(b) Detected voltage versus incident power.

Fig. 5: Back-scattering and Detection tests. The error bars show the dispersion for the four carriers.

The result of the test for the UL mode are depicted in Fig. 5a. In this second experimental verification the conversion gain is estimated measuring the sidebar reflected power normalized to the carrier power. The subcarrier is at 2 MHz, with a 2-PSK modulation at a data rate of 250 kbps. The experimental characteristic is flat up to -24 dBm: beyond this value the conversion gain is affected by a relevant compression.

The final test is a round-trip test which sums up both the UL and DL performance. The Frame Error Rate (FER) is estimated counting the valid packets during the exchange of 10^4 ECHO messages, at 5.7975 GHz. This test confirms the validity of the design, with a range exceeding 9 meters, as depicted in Fig. 6

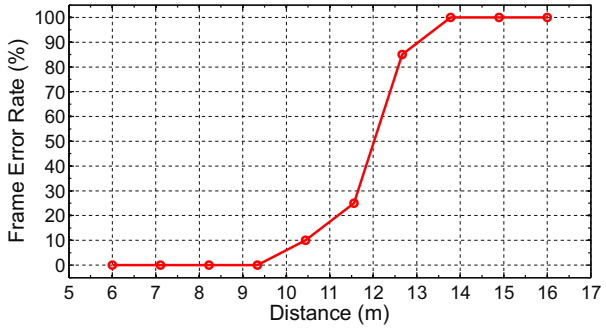

Fig. 6: Frame error rate of ECHO message at the RSU for the three prototypes; carrier at 5.7975 GHz.

VI. Conclusion

This paper has presented a prototype for a 5.8 GHz semi-passive transponder front-end for automotive applications complaint to ETSI EN300674. The proposed prototype is based on a design method already proposed by the authors, applied to a compact high gain antenna array. When integrated with an existent back-end processor, the resultant system demonstrates enhanced performance in both DL and UL cases, with a backscatteting gain of 7.8 dB, and a sensitivity of 54 mVpp, resulting in a enhanced range of 9 m when operating according to the condition dictated by ETSI EN300674 communication layer.

References

[1] *EN300674-1 V1.2.I, Electromagnetic compatibility and Radio spectrum Matters (ERM); Road Transport and Traffic Telematics (RTTT); Dedicated Short Range Communication (DSRC) transmission equipment (500 kbitls / 250 kbitls) operating in the 5,8 GHz Industrial, Scientific and Medical (ISM) band; Part 1: General characteristics and test methods for Road Side Units (RSU) and On-Board Units (OBU)*, ETSI.

[2] A. Cidronali, G. Collodi, M. Camprini, V. Nair, G. Manes, J. Lewis, and H. Goronkin, "Ultralow DC power VCO based on InP-HEMT and heterojunction interband tunnel diode for wireless applications," *Microwave Theory and Techniques, IEEE Transactions on*, vol. 50, no. 12, pp. 2938–2946, Dec 2002.

[3] S. Maddio, A. Cidronali, S. Maurri, and G. Manes, "Compact ETSI compliant DSRC transponder for vehicular communications at 5.8 GHz," in *Microwave Radar and Wireless Communications (MIKON), 2012 19th International Conference on*, vol. 1, May 2012, pp. 350–353.

[4] A. Aleksieieva and M. Vossiek, "Design and optimization of amplitude-modulated microwave backscatter transponders," in *German Microwave Conference, 2010*, March 2010, pp. 134–137.

[5] J. Meyer, Q. H. Dao, and B. Geck, "Design of an analog frontend for a 5.8 GHz RFID transponder," in *Microwave Conference Proceedings (APMC), 2012 Asia-Pacific*, Dec 2012, pp. 1043–1045.

[6] A. Cidronali, S. Maddio, G. Collodi, and G. Manes, "Design trade-off for a compact 5.8 GHz DSRC transponder front-end," *Microwave and Optical Technology Letters*, vol. 57, no. 5, pp. 1187–1191, 2015.

[7] R. Chakraborty, S. Roy, and V. Jandhyala, "Revisiting RFID link budgets for technology scaling: Range maximization of rfid tags," *Microwave Theory and Techniques, IEEE Transactions on*, vol. 59, no. 2, pp. 496–503, 2011.

[8] S. Maddio, A. Cidronali, and G. Manes, "A new design method for single-feed circular polarization microstrip antenna with an arbitrary impedance matching condition," *IEEE Transactions on Antennas and Propagation*, vol. 59, no. 2, pp. 379–389, 2011.

[9] S. Maddio, A. Cidronali, I. Magrini, and G. Manes, "A design method for single-feed wideband microstrip patch antenna for switchable circular polarization," *Microwave Conference, European*, pp. 262–265, 2007.

[10] U. R. Kraft, "An experimental study on 2 x 2 sequential-rotation arrays with circularly polarized microstrip radiators," *Antennas and Propagation, IEEE Transactions on*, vol. 45, no. 10, pp. 1459–1466, 1997.

[11] S. Maddio, "A Compact Wideband Circularly Polarized Antenna Array for C-band Applications," *Antennas and Wireless Propagation Letters, IEEE*, vol. 14, pp. 1081–1184, 2015.

[12] S. A. Maas, *Nonlinear microwave and RF circuits*. Artech House on Demand, 2003.

[13] A. Cidronali, K. Gupta, J. Jargon, K. A. Remley, D. DeGroot, and G. Manes, "Extraction of conversion matrices for p-hemts based on vectorial large-signal measurements," in *Microwave Symposium Digest, 2003 IEEE MTT-S International*, vol. 2, 2003, pp. 777–780 vol.2.

[14] R. Garg, *Microstrip Antenna Design Handbook*. Artech House, 2001.

[15] S. Maddio, A. Cidronali, and G. Manes, "An azimuth of arrival detector based on a compact complementary antenna system," in *Wireless Technology Conference (EuWIT), 2010 European*. IEEE, 2010, pp. 249–252.